8

MICROFLUIDIC FORMATION OF CELL-LADEN HYDROGEL MODULES FOR TISSUE ENGINEERING

YUYA MORIMOTO,[1,2] YUKIKO T. MATSUNAGA,[1,3] AND SHOJI TAKEUCHI[1,2]

[1] *Institute of Industrial Science (IIS), The University of Tokyo, Japan*

[2] *Takeuchi Biohybrid Innovation Project, ERATO, JST, Japan*

[3] *PRESTO, JST, Japan*

8.1 INTRODUCTION

Engineering of functional living tissues *in vitro* is important in regenerative medicine for generating transplantable grafts and pharmacokinetic studies. To engineer functional living tissues, cells need to be in the same environment as *in vivo*; *in vitro* tissues should mimic both the physical and the chemical properties of *in vivo* tissues.[1] *In vivo* tissues have three-dimensional (3D) hierarchical structures composed of various types of cells and extracellular matrices (ECMs). In these structures, cells receive mechanical stress and chemical stimuli from other cells and the surrounding ECMs.[2] These properties should be incorporated into engineered tissues to reconstruct an *in vivo*-like environment.

Hydrogels are commonly used for cell cultures because they are mostly a biocompatible, biodegradable, hydrophilic material and have a porous matrix.[3] These characteristics of hydrogels allow culturing of cells under relatively mild conditions. Moreover, because the size, shape, porosity, and chemical properties of hydrogels can easily be designed according to specific requirements, hydrogels are

Micro and Nanotechnologies in Engineering Stem Cells and Tissues, First Edition. Edited by Murugan Ramalingam, Esmaiel Jabbari, Seeram Ramakrishna, and Ali Khademhosseini.
© 2013 by The Institute of Electrical and Electronics Engineers, Inc. Published 2013 by John Wiley & Sons, Inc.

ideal materials for providing *in vivo*-like environments.[4] Therefore, hydrogels are useful for creating 3D cell structures.

Recently, microfabricated hydrogel modules are used as attractive microenvironments when culturing living cells; these hydrogel modules allow cells to attach on their surfaces or to be encapsulated (or both).[3,5] Such cell-laden hydrogel modules are mostly prepared by using microfludic devices because these devices can manipulate liquids in a controlled manner with high throughput, high uniformity, and design flexibility.[5–7] Because the size uniformity of the cell-laden hydrogel modules facilitates their handling, the modules are used in a wide range of applications, including the parallel analyses of cellular functions in the microfluidic analytical systems and the reconstruction of controlled-dense 3D cellular structures in "bottom-up" tissue engineering.[8,9]

This section provides an overview of (1) fabrication methods and characteristics of cell-laden hydrogel micromodules, (2) handling techniques of the modules in microfluidic devices, and (3) applications of the modules for transplantation and bottom-up tissue engineering.

8.2 CELL-LADEN HYDROGEL MODULES

This chapter introduces the reproducible fabrication methods of cell-laden hydrogel modules with a controllable design and the characteristics of the modules.

8.2.1 Types of Hydrogels

The favorable gelling mechanisms in microfluidic devices are ionic cross-linking with multivalent counterions, covalent cross-linking, and inherent phase transition such as heat of transition.[10] For example, hydrogels gelated under mild conditions are best suited to produce hydrogel modules for encapsulating cells. By selecting hydrogels with the appropriate gelling mechanism, hydrogel modules with the desired functions are obtained.

Hydrogels are mainly categorized into two types: hydrogels based on natural polymers and hydrogels based on synthetic polymers. Among the hydrogels obtained from natural polymers, collagen, hyaluronate, fibrin, alginate, and agarose are potentially attractive for tissue engineering applications. Collagen and hyaluronate are tissue-derived natural polymers and components of the ECMs. Collagen gelates in response to temperature change. Hyaluronate gelates by covalent cross-linking with hydrazide derivatives and radical polymerization of glycidyl methacrylate. Fibrin is a protein found in blood and gelates by the enzymatic polymerization of fibrinogen. Alginate and agarose are plant-derived natural polymers obtained from algae. Alginate gelates with divalent cations such as Ca^{2+} and Ba^{2+}. Agarose forms thermally reversible gels.

Among hydrogels obtained from synthetic polymers, poly(ethylene glycol) (PEG) and polypeptides have attractive potential applications. PEG gelates using by various methods, and a type of PEG is a photocross-linkable hydrogel. Moreover,

polypeptides are synthetic proteins that can mimic natural proteins. Genetically engineered polypeptides can be synthesized while controlling for their properties such as functions, stiffness, degradation, and cellular interactions. By considering the gelation, mechanical, and chemical properties of hydrogels, we can select suitable hydrogels for desirable applications.

8.2.2 Microfluidic Devices for Hydrogel Module Production

Many groups have demonstrated the production of hydrogel modules with high throughput and uniformity, and advances in microfluidic devices have resulted in various configurations of hydrogel modules such as blocks, beads, tubes, and sheets. The microfabrication techniques used for producing the hydrogel modules are reviewed in this section.

8.2.2.1 Hydrogel Beads A conventional method to produce hydrogel beads is emulsification. In this method, an immiscible liquid mixture of sol solution and oil with surfactants is stirred to generate small sol droplets.[11] The major disadvantages of emulsification are large-size distribution and more damage to encapsulated cells than the other approaches discussed here.

By using microfluidic devices, monodisperse and small sol droplets are produced. To generate sol droplets, quasi-two-dimensional (2D) planar microfluidic devices, such as T-junction microchannels[12,13] and 2D microfluidic flow-focusing devices,[14] are often used. In T-junction microchannels, monodisperse sol droplets can be formed at the T-junction facing two immiscible liquids such as a sol solution and oil including surfactants because the oil–surfactant mixture breaks the sol solution into droplets (Fig. 8.1a–c). In 2D flow-focusing devices, an inner fluid is broken into droplets by an outer fluid at the orifice or the downstream channel (Fig. 8.1d). When the sol solution is used as the inner fluid and oil with surfactants is used as the outer fluid, 2D flow-focusing devices produce monodisperse sol droplets. The droplet formation in both devices is driven by the Plateau–Rayleigh instability.[14,15] Therefore, droplet size is easily controlled on the basis of flow rates and channel dimensions. Additionally, both devices have the ability to produce sol droplets with high uniformity (coefficient of variation, CV) (<5%) and high throughput. However, the type of droplets that can be produced is dictated by the surface chemistry of the channel walls (i.e., hydrophobicity or hydrophilicity) because the inner fluid comes into direct contact with the channel walls; this phenomenon is known as the wetting problem. Therefore, sol droplets cannot be stably formed in hydrophilic channels because of the wetting problem. In some cases, fouling of channel surfaces by proteins and carbohydrate might make the formation of even sol droplets in hydrophobic channels difficult.[13] To circumvent the wetting problem, it is necessary to change the surface chemistry of 2D microfluidic channel walls (e.g., silanization) to cater for the desired usage.[16]

To avoid the wetting problem without any chemical modification, various 3D axisymmetric flow-focusing devices (AFFDs) have been developed to form monodisperse droplets.[17–20] In an AFFD, an inner fluid is surrounded by an outer fluid, and

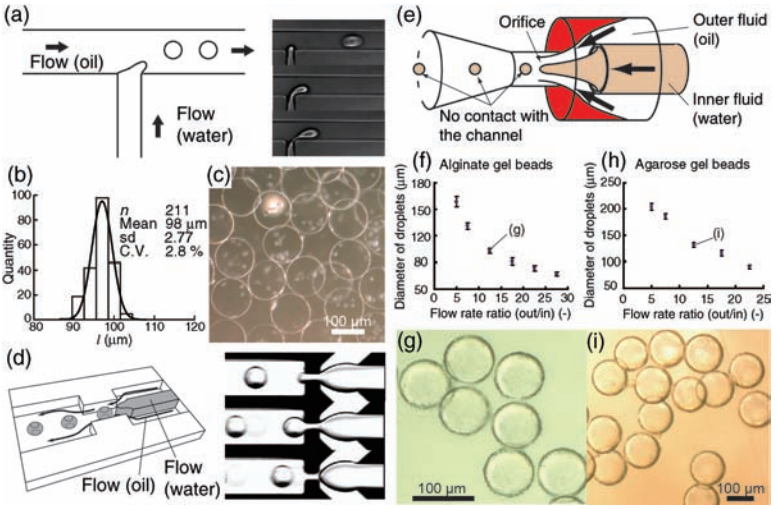

FIGURE 8.1 (a) Schematic illustration of the formation monodisperse droplets using the T-junction microchannel and images of droplet formation at the T-junction taken by a high-speed video camera. (b) Size distribution of the alginate gel beads produced by the T-junction device. The alginate gel beads show monodispersity (CV = 2.8%).[13] (c) Monodisperse alginate gel beads encapsulating Jurkat cells. The beads are also of a narrow size distribution.[13] (d) Schematic view of the 2D flow-focusing device and images of droplet formation in a flow-focusing device. In the 2D flow-focusing device, the droplets produced come into contact with the top and bottom of the channel walls. Therefore, the wetting problem occurs. (e) Schematic diagram of an AFFD used to produce monodisperse droplets. AFFDs can prevent droplets from adhering to the surface of the channels because the droplets are always surrounded by the outer fluid.[18] (f) Plot of the sizes of the alginate gel beads in the oil versus the flow rate ratio (outer flow rate/inner flow rate). CVs of every point are less than 5%, indicating all beads produced by the AFFD are monodisperse.[18] (g) Image of alginate gel beads in oil corresponding to (g) in figure (f).[18] (h–i) Formation of monodisperse agarose gel beads. The graph and images are in the same sequence as the alginate gel beads.[18] (e–i) Copyright (2009) Springer.

droplets are formed at the orifice or the downstream channel (Fig. 8.1e). The inner fluid and the produced droplets are always surrounded by an outer fluid, allowing the monodisperse droplets not to contact the channel walls, thus eliminating the wetting problem. The AFFD can control the size of droplets by adjusting flow rates and the orifice dimensions because droplet formation in an AFFD is controlled by the Plateau–Rayleigh instability (Fig. 8.1f–i).[17] Moreover, similar to 2D microfluidic devices, an AFFD can produce sol droplets with high uniformity and high throughput. After gelation of these monodisperse sol droplets produced by the microfluidic devices, monodisperse hydrogel microbeads are obtained.

Alternatively, monodisperse hydrogel microbeads are obtained using microjetting.[21] Using an inkjet printing technology, monodisperse sol droplets are produced in air, and the droplets are gelated to hydrogel microbeads by submerging them in an initiator of gelation. Also, the inkjet printing technology can organize hydrogel

microbeads into a layered formation in a solidifying gel with sequential hydrogel microbead fusion. The microjetting method can form not only hydrogel microbeads but also structures of other shapes, such as sheets and tubes, by stacking the hydrogel microbeads.

8.2.2.2 Hydrogel Blocks To produce hydrogel blocks, photolithography, flow lithography, and micromolding techniques are mainly used. Photolithography has a fast and high-resolution ($\sim$1 μm) performance in forming hydrogels with various shapes and sizes.[22] In the photolithography technique, the sol solution is initially molded into block shape and polymerized by using ultraviolet (UV) light. Because UV light triggers gelation, photocross-linkable microgels such as PEG should be used in this technique. The plane shape of the hydrogel blocks is obtained from the photomask design, and their depth follows the depth of the mold. Moreover, the plane shape of the depth direction can be controlled by changing the focus depth of UV light and the photomask patterns (Fig. 8.2a).[23] Therefore, photolithography can produce complicated structures such as polygons and rotundate blocks.

Alternatively, photolithography combined with microfluidics, so-called "flow lithography", allows the production of multifunctional hydrogel modules in continuous flow with high throughput.[24,25] Hydrogel blocks are fabricated in a microchannel by direct polymerization of UV light through a photomask. Then hydrogel blocks are obtained in continuous flow. The shapes of the hydrogel blocks are determined by the photomask patterns (Fig. 8.2b). In addition, computer-aided flow lithography is an advanced method to flow lithography.[26] In this technique, a computer controls the lighting areas to generate exposure patterns, and floating hydrogel blocks are obtained at arbitrary times and positions.

Micromolding is a simple method for producing hydrogel blocks with controlled features.[27] By using photolithography, silicon, glass, and polymer molds can be obtained in various sizes and shapes. Soft lithography has especially enabled the easy fabrication of poly(dimethylsiloxane) (PDMS) molds. To form hydrogel blocks of a variety of shapes and sizes, the sol solution is inserted into micromolds and subsequently gelated using an arbitrary gelling mechanism. The hydrogel blocks have high-resolution performance because the blocks transcribe the micromold patterns.

8.2.2.3 Hydrogel Fibers and Tubes Hydrogel fibers and tubes can be generated by cylindrical flow of solutions inside microfluidic devices. Transferring a cylindrical flow stream of a sol solution into an initiator of gelation can easily produce hydrogel fibers (Fig. 8.2c–e).[28] Also, hydrogel fibers are fabricated by coaxial microfluidic flows comprising a core flow surrounded by a sheath flow. When a sol solution and an initiator of gelation are introduced into the core flow and the sheath flow, respectively, a hydrogel fiber is formed.[29] Meanwhile, when a sample flow is concentrically located between the core flow and the sheath flow, hydrogel tubes are formed when the sol solution is inserted into the sample flow and the initiator of gelation is run into the core flow and the sheath flow (Fig. 8.2f and g).[30] The hydrogel fibers and tubes are formed without length limitation, and their diameter can be controlled by the flow

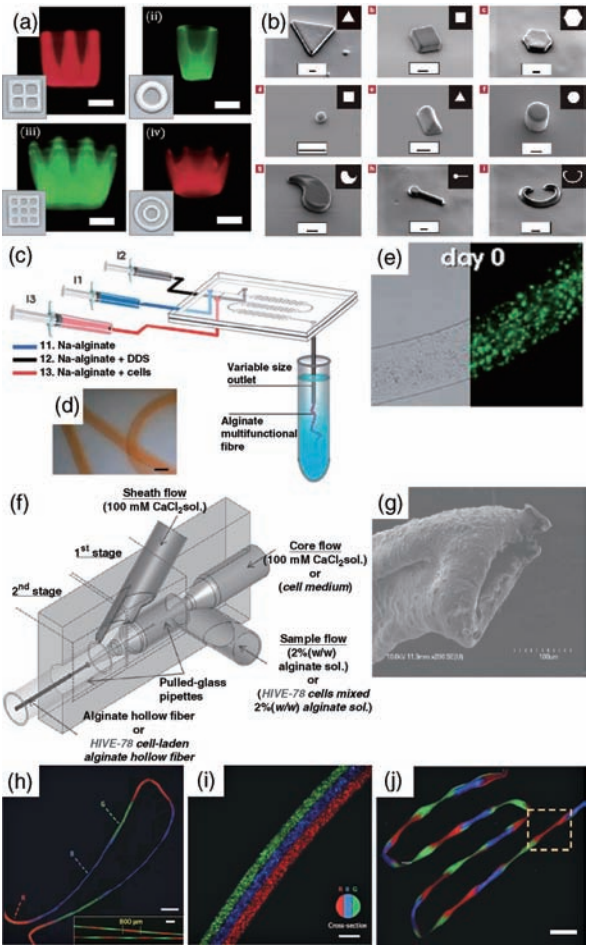

FIGURE 8.2 (a) Image of 3D-pattern hydrogel blocks fabricated by photolithography. The plane shape and depth of blocks are not only changed by the photomask design and the mold depth, respectively, but the plane shape of depth direction is also controlled by the altered focus depth of the UV light and light path. Scale bar, 50 μm.[23] (b) Image of hydrogel blocks formed by flow lithography. The shape of blocks can be easily varied according to the photomask design. The scale bar for all panels is 10 μm.[25] (c) Schematic fabrication procedure of hydrogel fibers.[28] (d) Image of the alginate fiber. Scale bar, 200 μm.[28] (e) Optical bright field and fluorescence image of alginate fiber containing Wharton's jelly mesenchymal stem cells.[28] (f) Schematic diagram of the microfluidic device that generates the alginate gel tubes. Coaxial flow composed of core and sample flows is generated, and gelling of the alginate sol in the sample flow starts at the interface of both flows. After the sheath flow surrounds the coaxial flow, solidification occurs simultaneously at the interface between the sample flow and the sheath flow.[30] (g) Scanning electron microscopic image of the hydrogel tube.[30] (h) Image of serially coded fiber and its close-up image. Scale bars, 1 mm and 400 μm (close-up image).[31] (i) Image of parallel coded fiber. Scale bar, 200 μm.[31] (j) Image of a fiber with spatiotemporal variations in morphology and chemical composition. Scale bar, 1 mm.[31] (h–j) Each type of fluorescent polystyrene beads emits different colors: red, blue, and green. (a) Copyright 2011 Royal Society of Chemistry, (b) copyright 2006 Nature Publishing Group, (c–e) copyright 2011 Royal Society of Chemistry, (f, g) copyright 2009 John Wiley and Sons, and (h–j) copyright 2011 Nature Publishing Group.

rates and channel dimensions. In addition, by combining the fabrication techniques of hydrogel fibers and air valves, hydrogel fibers coded with varying chemical compositions and topographies along the fibers are generated (Fig. 8.2h–j).[31] Using this method, hydrogel fibers encapsulating multiple and spatially controlled cells can be created for tissue engineering applications.

8.3 CELL ASSAY SYSTEMS USING MICROFLUIDIC DEVICES

Because of their size uniformity, the cell-laden hydrogel modules are manipulated as monodisperse beads. Therefore, these modules can be handled, arrayed, and retrieved using microfluidic bead-based assay systems for accurate analyses. The characteristics of microfluidic devices for handling hydrogel modules and their potential for use in analysis of cell biological systems are reviewed in this section.

8.3.1 Microfluidic Devices for Handling Modules

Cell-based microfluidic devices can provide precise spatial and temporal control of samples and reagents, which is difficult to achieve using 2D cell culture systems. Moreover, they allow real-time monitoring and analysis of samples in order to obtain insight into cell dynamics. Microarray systems especially have extensive applications for drug discovery and diagnostic and basic scientific studies.

8.3.1.1 Microwell Devices Microwell devices have a simple mechanism to trap samples statically in an array.[32,33] They allow samples to sink into microwells and hold a sample in each microwell. Microwell devices are fabricated accurately using a variety of technologies such as photolithography. Microwells have the advantage of having a massively parallel format (>10000) and allowing the observation of all samples from the same direction. In addition, microwells are suitable for trapping a single sample in almost all microwells by adjusting the well diameters and depths. Therefore, microwell devices are used to screen samples for drug kinetics studies.

8.3.1.2 Hydrodynamic Microarray Devices Hydrodynamic microarray devices are commonly used for trapping samples in microfluidic systems. The following are the advantages of hydrodynamic microarrays over microwell devices: hydrodynamic microarrays allow transporting of samples, immobilizing of samples for convenient analysis, delivering reagents to samples with continuous observation, and retrieving of selected samples.

The most common way to immobilize samples in microfluidic systems is to arrange the side channels in a main channel.[34] When the diameter of the side channel is sufficiently small, samples are trapped by suction because the sidestream from the main channel runs samples into the side channel. The hydrodynamic systems are capable of releasing samples as the sidestream is reversed. Also, using hydrodynamic trapping holes, similar to the microwells, samples can be immobilized and retrieved

in large quantities. Thus, hydrodynamic microfluidic devices have an attractive potential for trapping and analyzing samples.

Single sample-trapping systems with individual addressing are developed using advanced microfluidics strategies;[35,36] meander-shaped hydrodynamic microfluidic devices are a representative example.[37,38] A meander-shaped hydrodynamic microfluidic device is composed of a meander-shaped main channel and a trapping region with a narrow, straight channel (Fig. 8.3a and b). The straight channel has lower flow resistance than the main channel when samples are not trapped. This phenomenon causes the bulk of the fluid to flow along the straight channel, and samples in the main stream are delivered into all trapping regions. Also, the meander-shaped hydrodynamic microfluidic device can retrieve a trapped sample (Fig. 8.3c). A laser setup to heat a localized area results in selective microbubble formation near the trapping area, and the expanding microbubble pushes the immobilized sample into the main stream. In the device, samples are selectively released, and the displaced samples can be collected by allowing them to flow out of the device. Moreover, a resettable configuration added to the meander-shaped hydrodynamic microfluidic device allows the release of all the trapped samples without clogging the device when the flow direction is reversed.[39]

8.3.2 Cell Analysis Using Microfluidic Devices

Using microfluidic devices, samples can be transported, immobilized, and observed continuously. For example, owing to the meander-shaped hydrodynamic microfluidic devices, monodisperse hollow alginate capsules coated with poly-L-lysine (PLL) containing motile cells can be immobilized and arrayed (Fig. 8.3d).[40] The hollow and semipermeable capsules facilitate the continuous observation of encapsulated arrayed motile cells while preventing invasion of other cells and allowing the exchange of nutrients and wastes.

Also, microfluidic devices allow investigating cells in 3D culture conditions. Cellular signals are sometimes changed in cells cultured on a flat substrate because cells adhered on a 2D substrate lack structural cues. Therefore, cell analyses in 3D culture systems are important for accurately understanding cell biology. Cell-laden hydrogel modules are a useful 3D culture model system because of their stable size, shape, and cell density. In addition, ECMs can be used as cell-encapsulating materials to construct tissue-like microstructures. Monodisperse alginate gel beads encapsulating Jurkat cells fabricated by the T-junction microchannel, and monodisperse collagen gel beads seeded with fibroblast cells (3T3 cells) formed by AFFD have been delivered and arrayed using a meander-shaped microfluidic channel.[38,41] Specifically, live-dead assay of fibroblast cells on collagen gel beads can be performed in a microfluidic channel during the beads trapping. In addition, a coculture assay system for constructing cell–cell interaction among different types of cells has also been realized in an improved meander-shaped microfluidic channel (Fig. 8.3e and f).[42] Because the channel can trap and pair different types of beads, the system would be applicable for continuous observation of cell–cell interactions between paired cell-laden hydrogel beads.

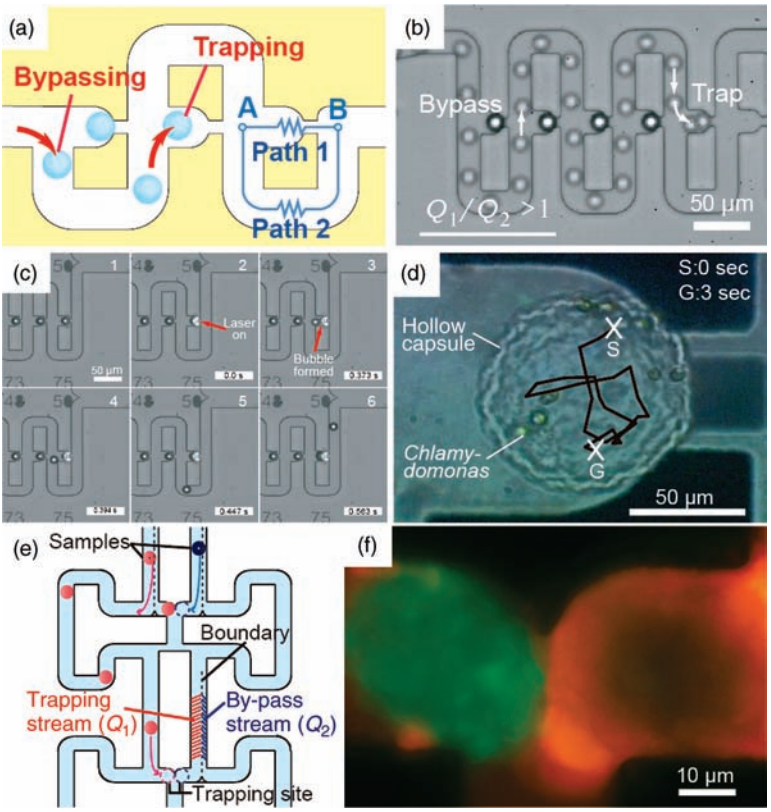

FIGURE 8.3 (a) Schematic diagram of a meander-shaped hydrodynamic microfluidic device. When the trapping area is empty, a bead in the mainstream is delivered into the trapping area. When the trapping area is full, beads are carried along the meander-shaped main channel.[37] (b) Superimposed time-lapsed high-speed camera image showing the trapped beads.[37] (c) Sequence images taken by a high-speed camera indicating the retrieval of beads using bubbles.[37] (d) Image of monodisperse hollow capsules comprising a PLL-alginate membrane and the encapsulating microbe, *Chlamydomonas*. The path traced by *Chlamydomonas* in 3 s is shown. The image shows that the motility of the encapsulated microbes is not compromised inside the hollow capsule. In addition, continuous observation was carried out for more than 2 h.[40] (e) Schematic view of the improved meander-shaped hydrodynamic device that allows different types of hydrogel beads to be paired.[42] (f) Fluorescent images of collagen gel beads with stained cells paired with different types of cells. *Red* indicates HepG2 cells and *green* indicates 3T3 cells.[42] (d) Copyright 2009 Royal Society of Chemistry and (e, f) copyright 2010 Royal Society of Chemistry.

8.4 IMPLANTABLE APPLICATIONS

Successful cell transplantation without immunosuppression might be achieved by immunoisolation through hydrogel encapsulation. The characteristics of cell-laden

hydrogel modules for transplantation and implantable applications are reviewed in this section.

8.4.1 Cell-Laden Hydrogel Modules for Transplantation

The approach for the immunoisolation of encapsulated cells uses a semipermeable membrane made from hydrogels. The membrane forms a mechanical barrier separating encapsulated cells from the host antibodies (>150 kDa) and immune cells but allows the diffusion of small molecules (<10 kDa) such as glucose, insulin, nutrients, and cell waste products.[43] Cells encapsulated into hydrogel beads are commonly used for implantation. Their spherical shape enables sufficient diffusion of nutrients and cell products because the bead shape have a better surface–volume ratio than materials of any other shape. Additionally, hydrogel beads cannot be easily disrupted, are mechanically stable, are reproducible by microfluidics methods, and can be implanted into the patient by a simple injection procedure.

Hydrogels for use in transplantation need to be immunoisolated and capable of diffusing nutrients and cell products. Alginate, agarose, and chitosan as natural polymers, and poly(hydroxyethyl methacrylate-methyl methacrylate) (HEMA-MMA), acrylonitrile, and PEG as synthetic polymers have reported uses for cell encapsulation in hydrogels.[44,45] Alginate-based beads are mainly preferred because alginate does not interfere with cellular functions and can keep arbitrary shapes.[46]

The fabrication process of alginate beads can be broadly classified into two categories: external gelation and internal gelation.[15] In the external gelation method, Na-alginate droplets are gelated by the external addition of divalent cations. For example, in the production of Ca-alginate beads, Na-alginate droplets are transferred into a calcium chloride ($CaCl_2$) solution. The rapid gelling behavior of alginate in the external gelation method makes it difficult to produce well-defined, homogeneous, and monodisperse alginate hydrogel beads. On the other hand, the internal gelation method involves dispersing an insoluble (or slowly soluble) complex in the Na-alginate solution.[47] Because of pH reduction, divalent cations are released from the complex, cross-linking the alginate to form homogeneous and monodisperse hydrogel beads.

The type of divalent cations cross-linking the alginate also contributes to the morphology of the alginate gel and the viability of the encapsulated cells. Ca ions are suited for the production of perfectly spherical and stable alginate beads. However, Ca ions have toxic effects, and encapsulated cells are damaged when they are exposed to Ca ions for a prolonged time. Ba ions react with alginate in a stronger way compared with Ca ions. Although Ba ions have high biocompatibility and cells encapsulated in Ba-alginate beads show high viability, Ba-alginate beads are easily deformable.[48]

8.4.2 Implantable Applications of Cell-Laden Hydrogel Modules

Hydrogel beads are used in cell transplantation (Fig. 8.4a): various types of cells (e.g., islet and Sertoli cells) encapsulated in alginate beads are transplanted into

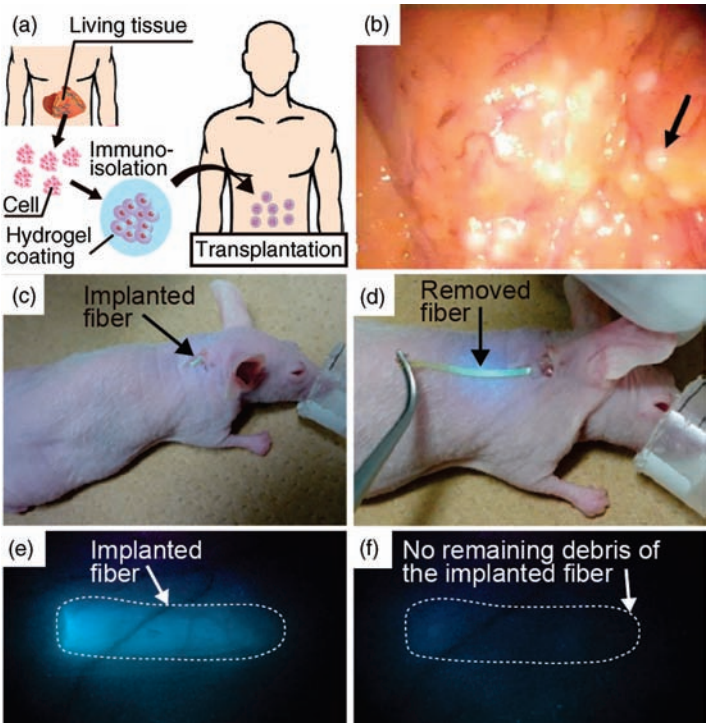

FIGURE 8.4 (a) Schematic diagram of transplantation using cell-laden hydrogel modules. Because hydrogel protect the invasion of immune antibodies, encapsulated cells can live for a long time without immune reactions. (b) Laparoscopic view of the omentum of a patient with type 1 diabetes 9 years after transplantation of alginate capsules encapsulating porcine islets.[49] (c) Fiber is implanted in the mouse ear to continuously monitor the glucose level.[50] (d) The implanted fiber is easily removed from the ear.[50] (e) Fluorescent image of the mouse ear containing the fiber. The fiber transmits fluorescent signals continuously depending on blood glucose concentration.[50] (f) Fluorescent image of the mouse ear after fiber removal. The image shows that the implanted fibers are retrieved from the ear without leaving debris.[50] (b) Copyright 2007 John Wiley and Sons.

living organisms. Encapsulation of cells protects them from immune antibodies and mechanical stress, so the cells remain viable for a long time (>1 year) after the transplantation.[48] Moreover, because the encapsulated cells express the cellular functions, alginate-based beads containing cells have potential to be considered as new therapeutic devices. For instance, islet cells encapsulated in alginate beads can control blood glucose levels *in vivo* for a long period and thus show potential to provide treatment for patients with diabetes (Fig. 8.4b).[49]

Recently, cells encapsulated in hydrogel tubes and fibers have been proposed.[28,30,31] The fibers and tubes have advantages over beads for long-term implantation *in vivo* (i.e., they can remain at the implantation space for a long period, but beads disperse from the implantation area). Also, fibers and tubes can be

easily and nonsurgically removed from the body by withdrawing their end portions. In addition, use of hydrogel fibers encapsulating a fluorescent gel indicates changes of glucose concentration (Fig. 8.4c–f).[50] By implanting the fibers, the glucose level can continuously be monitored *in vivo*. This shows the potential of hydrogel fibers and tubes for implantation, encapsulating not only cells but also various functional products.

Cell sheets are formed by incubating cells on a hydrogel layer that is used to detach the cells from a substrate. In particular, using a poly(*N*-isopropylacrylamide) (PNIPAAm) layer is a potentially powerful method for generating cell sheets.[51] Because PNIPAAm has a low critical solution temperature of 32°C and cells detach from the PNIPAAm layer under this temperature, cells cultured on a PNIPAAm sheet can be harvested as cell sheets along with their deposited ECM. Because the cell sheets keep the ECM on their basal surface, they can be transplanted directly to host tissues. Cell sheets have potential applications for cell-based regenerative therapies.[52] Transplantation of a single cell sheet into a host tissue can reconstruct corneal epithelium, skin, bladder urothelium, and periodontal ligaments. By homotypic layering of cell sheets, 3D tissue structures such as cardiac and smooth muscles can be recreated. With heterotypic stratification of various cell sheets, more complex and higher ordered laminar structures such as liver lobules and kidney glomeruli can be constructed. The use of cell sheets allows attaching cells to host wound tissues without loss of some cells.

8.5 TISSUE ENGINEERING

A demand currently exists for constructing macroscopic 3D tissue architectures that mimic tissue structures *in vivo* for repairing injured, degenerated, and inherently defective tissues. There are two different approaches for tissue engineering: the top-down approach and the bottom-up approach. The top-down approach uses 3D scaffolds with the desired tissue architecture.[53] In contrast, the bottom-up approach uses microtissue units as building blocks.[9] Microtissue units are powerful tools for reconstructing organomimetic and homogeneous dense structures. By molding microtissue units, uniform and arbitrarily shaped tissues can be fabricated without necrosis.

8.5.1 Microtissue Units

Microtissue units based on hydrogel modules are applicable for microscopic tissue engineering. One approach uses hydrogel modules encapsulating cells and covered by another type of cells. This method achieves formation of a hierarchical 3D coculture system for fabrication of microscopic tissues and heterotypic cellular interactions under 3D coculture conditions (Fig. 8.5a and b).[41,54] Because cellular functions are increased in the 3D coculture microtissues, microtissue-based hydrogel modules are useful for high-throughput studies of pathological and physiological phenomena in 3D coculture cells.

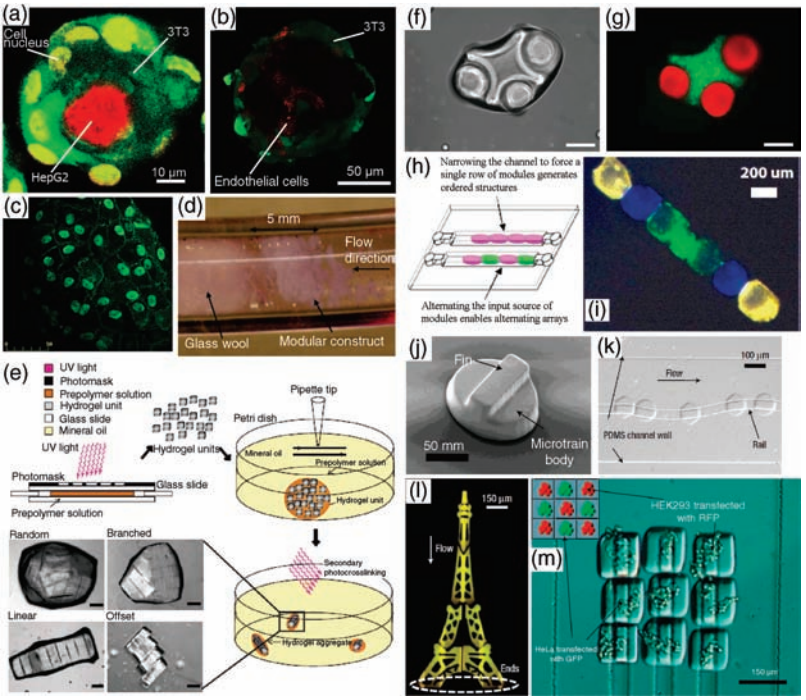

FIGURE 8.5 (a, b) Fluorescence confocal microscopy of hierarchical cocultured cell beads. (a) Collagen gel beads encapsulating HepG2 cells (red) and seeded with 3T3 cells (green) after 17 h of incubation.[41] (b) Self-assembling peptide beads containing endothelial cells (red) and 3T3 cells (green) after 2 days of culture.[54] (c) Fluorescent image of a collagen gel rod seeded with HUVEC cells showing the rod covered with a confluent cell layer.[55] (d) Image of the modular construct, including the microporous body.[55] (e) Schematic suggesting assembly of cell-laden hydrogel blocks in oil. Mechanical agitation applied using a pipette tip and secondary cross-linking form diverse shapes of gel assemblies: random, branched, linear, and offset.[56] (f, g) Images of the lock-and-key-shaped gel assembly containing three rods per cross. Cross-shaped gel and rod-shaped gel encapsulates red-labeled and green-labeled 3T3 cells, respectively. Scale bars, 200 μm.[56] (h) Schematic diagrams of the assembly of cell-laden hydrogel blocks to form lined-shaped cell structures in a microfluidic device.[57] (i) Image of the line-shaped cell structure consisting of three differently labeled cells.[57] (j) Scanning electron microscope image of the microtrain.[58] (k) Guided movement of microtrain along a reentrant rail.[58] (l) Image of the Eiffel Tower assembly produced by the guided assembly method.[58] (m) Image of the rail-guided assembly including two different types of living cells. *Green* and *red* indicate HeLa and HEK293 cells, respectively.[58] (c, d) Copyright 2006 National Academy of Science, (e–g) copyright 2008 National Academy of Science, (h, i) copyright 2008 Royal Society of Chemistry, (j–m) copyright 2008 Nature Publishing Group.

8.5.2 Random Assembly of Microtissue Units

Random assemblies of microtissue units result in vascularized tissues (Fig. 8.5c and d).[55] For this application, collagen gel rods seeded with endothelial cells (HUVEC cells) and encapsulating hepatocyte cells (HepG2 cells) are used. After preparing rod-shaped collagen gels encapsulating hepatocyte cells, endothelial cells are spread on the gel and cultured until a confluent layer of endothelial cells grows on the surface of the gel. The rod-shaped HUVEC-HepG2 microtissues are assembled into a larger tube with perfusion of medium or whole blood. The perfusion induces remodeling of cells and produces a perfusable tissue with a microporous body because the spaces between microtissues become microchannels. The simple method using a random assembly creates functional tissue equivalents and potentially engineer organ grafts.

8.5.3 Controlled Assembly of Microtissue Units

In contrast to random assembly, a controlled assembly method can make arbitrarily shaped tissues. In this method, the surface tension force at the water–oil interface is used to aggregate hydrogel blocks (Fig. 8.5e–g).[56] First, PEG-methacrylate (PEGmA) gel blocks containing cells are produced by photolithography using UV light. After gelling, the PEGmA gel blocks soaked in sol solution are transferred into mineral oil, where the gel blocks are assembled by mechanical agitation. Subsequently, exposure to UV light gelates the gel blocks into assembly. This method also generates 3D cell structures containing multiple types of cells. In particular, lock-and-key assemblies composed of cross-shaped gel blocks and plural rod-shaped gel blocks form coculture tissues without any additional steps. Using this method, the tissues formed from microtissue units are fabricated reproducibly without complicated assembly and handling procedures.

In the approach using microfluidic devices, collagen blocks containing cells fabricated by a micromolding method are assembled into microchannels or microchambers (Fig. 8.5h–i).[57] When assembling collagen blocks in microchambers, 3D cell structures are generated, but hydrodynamics in the narrow microchannel forces the collagen blocks to produce ordered structures. The advantage of this method lies in its ability to form tissue structures containing multiple types of cells. The 3D cell-lined structure comprising hierarchical coculture tissues will allow studying 3D cell–cell interactions and signaling.

In another approach, convex PEG gel blocks, microtrains, are produced by flow lithography and are fluidically assembled along a concave rail (Fig. 8.5i and k).[58] Using the rails as guides, complex 2D structures are built by fluidically assembling microtrains with zero error and incorporating all microtrains as components in the structures (Fig. 8.5l). Furthermore, heterogeneous fluidic assembly of microtrains containing different types of living cells is achieved by the same guiding mechanism (Fig. 8.5m). The guided and fluidic assembly method require the convex hydrogel blocks and the concave rails but has strong potential, owing to its flexibility, to produce heterogeneous and complex cell-laden structures as living tissues.

8.5.4 Macroscopic Assembly of Microtissue Units

Although various approaches using cell-laden hydrogel modules provide 3D cell structures, formation of a large-scale macroscopic tissue structure has been difficult because of the size, uniformity, and throughput limitations of hydrogel modules. One method of engineering macroscopic tissue structures is proposed as a solution: a random assembly approach consisting of monodisperse cell-laden collagen gel beads to achieve a rapid construction of millimeter-thick complex macroscopic tissues (Fig. 8.6a–c).[41] The tissue fabrication process uses monodisperse collagen gel beads fabricated by an AFFD and covers them with cells (namely, "cell beads"). The cell

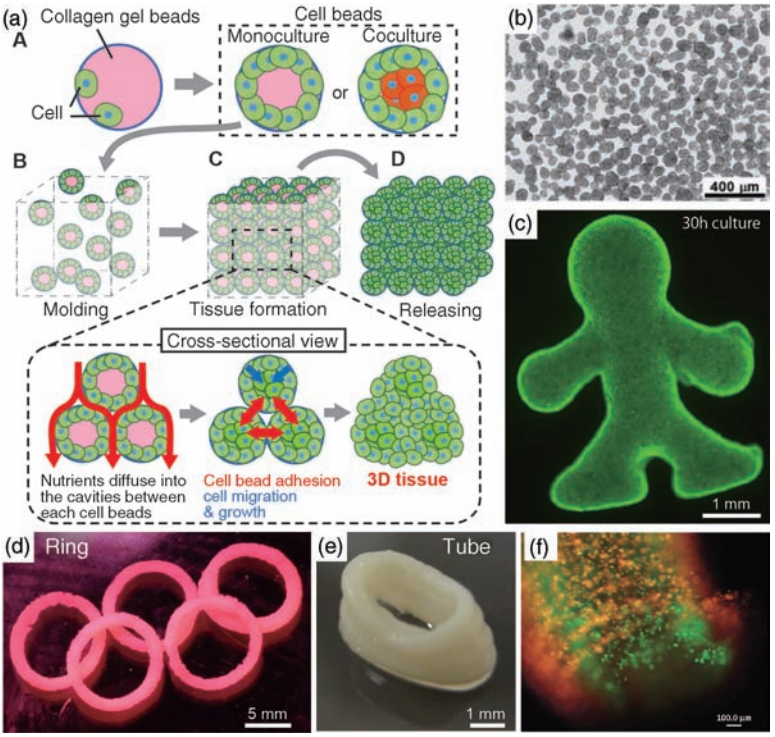

FIGURE 8.6 (a) Concept of bead-based tissue engineering: monodisperse cell beads are molded into a macroscopic cell structure.[41] (A, B) Monodisperse cell beads are poured into a designed PDMS mold. (C) During tissue formation, the medium diffuses inside the 3D cell structures via the cavities of the cell beads, supplying nutrients to all cells. (D) Macroscopic 3D cell structures are released from the PDMS mold. (b) Image of cell beads seeded with 3T3 cells; they are the building modules for the construction of a macroscopic 3D cell culture.[41] (c) Fluorescent image of the macroscopic structures having a complicated shape. Live-dead assay staining indicates that almost all cells within the structure are alive.[41] (d, e) Ring- and tube-shaped cell structures fabricated by the printing method.[41] (f) Tube-shaped hierarchical coculture structures made from printing cells. The inner layer is composed of human umbilical endothelial cells (green), and the outer layer is composed of human aortic smooth muscle cells (red). Image provided by Prof. Nakamura, Toyama University, Japan.

beads are then molded into a designed PDMS chamber to construct the macroscopic 3D tissue structure. In the chamber, the cells grow and migrate into the body of the beads by degrading collagen, and the cell beads adhere to each other via the cells enclosing the collagen gel beads, resulting in macroscopic 3D tissue structures. Finally, the fabricated tissue is removed from the PDMS mold. This method features the rapid production of macroscopic 3D tissue structures, a homogeneous cell density, and tissue formation without necrosis during less than 1 week because the cell culture medium can be supplied via the cavities between each cell bead and from the collagen. These characteristics make the method compatible with other 3D tissue engineering tasks because cell beads containing various types of cells can be easily assembled and aligned to generate macroscopic 3D structures with any desired shape.

The printing method is useful for a macroscopic controlled assembly approach for engineering 3D structures.[59] Printing generates microtissue unit composed of cells within hydrogels. In contrast to microtissue units fabricated by photolithography and flow lithography, printing can stack cells within hydrogels in layered form to construct 3D tissue structures. The advantage of the printing approach is the fast construction of 3D tissue structures with control of cell placement and structure geometries. Also, the printing method can create complex-shaped structures such as hollow-tube tissues (Fig. 8.6d and e).[41,60] Moreover, because the printing method can accurately control the location of cells in patterns, hierarchical tube structures containing two different types of cells are obtained (Fig. 8.6f).[61] Using the printing method, 3D structures containing various types of cells are built into the tissue matrix in a simple and versatile way.

8.6 SUMMARY

Microfluidic techniques succeed in reproducibly constructing diversely shaped hydrogel modules such as beads, blocks, fibers, tubes, and sheets with high throughput, high uniformity, and design flexibility. These hydrogel modules have applications in various fields ranging from basic biology studies to tissue engineering. Combined with cell assay microfluidic systems and cell-laden hydrogel modules, microtissues with ECM are useful for analyses of cell functions and cell–cell interactions because microtissues can easily be handled, arrayed, and retrieved in microfluidic systems. Furthermore, the cell-laden hydrogel modules can be used as building units for reconstructing 3D cell structures. Therefore, the cell-laden hydrogel modules produced by microfluidic devices have a great potential to create miniaturized tissues for human implantation and for treatment of diseases.

REFERENCES

1. Pampaloni F, Reynaud EG, Stelzer EHK. The third dimension bridges the gap between cell culture and live tissue. Nat Rev Mol Cell Biol 2007;8(10):839–845.

2. Albrecht DR, Underhill GH, Wassermann TB, Sah RL, Bhatia SN. Probing the role of multicellular organization in three-dimensional microenvironments. Nat Methods 2006;3 (5):369–375.
3. Khademhosseini A, Langer R. Microengineered hydrogels for tissue engineering. Biomaterials 2007;28(34):5087–5092.
4. Drury JL, Mooney DJ. Hydrogels for tissue engineering: scaffold design variables and applications. Biomaterials 2003;24(24):4337–4351.
5. Chung BG, Lee KH, Khademhosseini A, Lee SH. Microfluidic fabrication of microengineered hydrogels and their application in tissue engineering. Lab Chip 2011;12 (1):45–59.
6. Peppas NA, Hilt JZ, Khademhosseini A, Langer R. Hydrogels in biology and medicine: from molecular principles to bionanotechnology. Adv Mater 2006;18(11):1345–1360.
7. Griffiths AD, Tawfik DS. Miniaturising the laboratory in emulsion droplets. Trends Biotechnol 2006;24(9):395–402.
8. Nilsson J, Evander M, Hammarstrom B, Laurell T. Review of cell and particle trapping in microfluidic systems. Anal Chim Acta 2009;649(2):141–157.
9. Elbert DL. Bottom-up tissue engineering. Curr Opin Biotechnol 2011;22:1–7.
10. Lee KY, Mooney DJ. Hydrogels for tissue engineering. Chem Rev 2001;101(7):1869–1879.
11. Dulieu C, Poncelet D, Neufeld RJ. Encapsulation and immobilization techniques. *In: Cell Encapsulation Technology and Therapeutics*. Boston: Birkhauser;1999; pp. 3–17.
12. Thorsen T, Roberts RW, Arnold FH, Quake SR. Dynamic pattern formation in a vesicle-generating microfluidic device. Phys Rev Lett 2001;86(18):4163–4166.
13. Tan WH, Takeuchi S. Monodisperse alginate hydrogel microbeads for cell encapsulation. Adv Mater 2007;19:26962701.
14. Anna SL, Bontoux N, Stone HA. Formation of dispersions using "flow focusing" in microchannels. Appl Phys Lett 2003;82(3):364–366.
15. Link DR, Anna SL, Weitz DA, Stone HA. Geometrically mediated breakup of drops in microfluidic devices. Phys Rev Lett 2004;92(5):054503.
16. Okushima S, Nisisako T, Torii T, Higuchi T. Controlled production of monodisperse double emulsions by two-step droplet breakup in microfluidic devices. Langmuir 2004;20 (23):9905–9908.
17. Utada AS, Lorenceau E, link DR, Kaplan PD, Stone HA, Weitz DA. Monodisperse double emulsions generated from a microcapillary device. Science 2005;308(5721):537–541.
18. Morimoto Y, Tan WH, Takeuchi S. Three-dimensional axisymmetric flow-focusing device using stereolithography. Biomed Microdevices 2009;11(2):369–377.
19. Morimoto Y, Kuribayashi-Shigetomi K, Takeuchi S. A hybrid axisymmetric flow-focusing device for monodisperse picoliter droplets. J Micromech Microeng 2011;21 (5):054031.
20. Takeuchi S, Garstecki P, Weibel DB, Whitesides GM. An axisymmetric flow-focusing microfluidic device. Adv Mater 2005;17(8):1067–1072.
21. Nakamura M, Nishiyama Y, Henmi C, Iwanaga S, Nakagawa H, Yamaguchi K, Akita K, Mochizuki S, Takiura K. Ink jet three-dimensional digital fabrication for biological tissue manufacturing: analysis of alginate microgel beads produced by ink jet droplets for three dimensional tissue fabrication. J Imaging Sci Technol 2008;52(6):060201.

22. Liu VA, Bhatia SN. Three-dimensional photopatterning of hydrogels containing living cells. Biomed Microdevices 2002;4(4):257–266.
23. Kim LN, Choi S-E, Kim J, Kim H, Kwon S. Single exposure fabrication and manipulation of 3D hydrogel cell microcarriers. Lab Chip 2011;11(1):48–51.
24. Panda P, Ali S, Lo E, Chung BG, Hatton TA, Khademhosseini A, Doyle PS. Stop-flow lithography to generate cell-laden microgel particles. Lab Chip 2008;8(7):1056–1061.
25. Dendukuri D, Pregibon DC, Collins J, Hatton TA, Doyle PS. Continuous-flow lithography for high-throughput microparticle synthesis. Nat Mater 2006;5(5):365–369.
26. Lee H, Kim J, Kim H, Kim J, Kwon S. Colour-barcoded magnetic microparticles for multiplexed bioassays. Nat Mater 2010;9(9):745–749.
27. McGuigan AP, Bruzewicz DA, Giavan A, Butte M, Whitesides G. Cell encapsulation in sub-mm sized gel modules using replica molding. PLoS ONE 2008;3(5):e2258.
28. Mazzitelli S, Capretto L, Carugo D, Zhang X, Piva R, Nastruzzi C. Optimised production of multifunctional microfibres by microfluidic chip technology for tissue engineering applications. Lab Chip 2011;11(10):1776–1785.
29. Hwang CM, Khademhosseini A, Park Y, Sun K, Lee SH. Microfluidic chip-based fabrication of PLGA microfiber scaffolds for tissue engineering. Langmuir 2008;24 (13):6845–6851.
30. Lee KH, Shin SJ, Park Y, Lee SH. Synthesis of cell-laden alginate hollow fibers using microfluidic chips and microvascularized tissue-engineering applications. Small 2009;5 (11):1264–1268.
31. Kang E, Jeong GS, Choi YY, Lee KH, Khademhosseini A, Lee SH. Digitally tunable physicochemical coding of material composition and topography in continuous microfibres. Nat Mater 2011;10(11):877–883.
32. Rettig JR, Folch A. Large-scale single-cell trapping and imaging using microwell arrays. Anal Chem 2005;77(17):5628–5634.
33. Lee WC, Rigante S, Pisano AP, Kuypers FA. Large-scale arrays of picolitre chambers for single-cell analysis of large cell populations. Lab Chip 2010;10(21):2952–2958.
34. Yang M, Li CW, Yang J. Cell docking and on-chip monitoring of cellular reactions with a controlled concentration gradient on a microfluidic device. Anal Chem 2002;74 (16):3991–4001.
35. Di Carlo D, Aghdam N, Lee LP. Single-cell enzyme concentrations, kinetics, and inhibition analysis using high-density hydrodynamic cell isolation arrays. Anal Chem 2006;78(14):4925–4930.
36. Skelley AM, Kirak O, Suh H, Jaenisch R, Voldman J. Microfluidic control of cell pairing and fusion. Nat Methods 2009;6(2):147–152.
37. Tan WH, Takeuchi S. A trap-and-release integrated microfluidic system for dynamic microarray applications. Proc Natl Acad Sci USA 2007;104(4):1146–1151.
38. Tan WH, Takeuchi S. Dynamic microarray system with gentle retrieval mechanism for cell-encapsulating hydrogel beads. Lab Chip 2008;8(2):259–266.
39. Iwai K, Tan WH, Ishihara H, Takeuchi S. A resettable dynamic microarray device. Biomed Microdevices 2011;13(6):1089–1094.
40. Morimoto Y, Tan WH, Tsuda Y, Takeuchi S. Monodisperse semi-permeable microcapsules for continuous observation of cells. Lab Chip 2009;9:2217–2223.
41. Matsunaga YT, Morimoto Y, Takeuchi S. Molding cell beads for rapid construction of macroscopic 3D tissue architecture. Adv Mater 2011;23(12):H90–H94.

42. Teshima T, Ishihara H, Iwai K, Adachi A, Takeuchi S. A dynamic microarray device for paired bead-based analysis. Lab Chip 2010;10(18):2443–2448.
43. Schneider SW, Larmer J, Henderson RM, Oberleithner H. Molecular weights of individual proteins correlate with molecular volumes measured by atomic force microscopy. Pflugers Arch 1998;435(3):362–367.
44. de Vos P, Hamel AF, Tatarkiewicz K. Considerations for successful transplantation of encapsulated pancreatic islets. Diabetologia 2002;45(2):159–173.
45. Klein J, Stock J, Vorlop KD. Pore-size and properties of spherical Ca-alginate biocatalysts. Eur J Appl Microbiol Biotechnol 1983;18(2):86–91.
46. Poncelet D. Production of alginate beads by emulsification/internal gelation. Ann N Y Acad Sci 2001;944:74–82.
47. de Vos P, Faas MM, Strand B, Calafiore R. Alginate-based microcapsules for immunoisolation of pancreatic islets. Biomaterials 2006;27:5603–5617.
48. Luca G, Calvitti M, Nastruzzi C, Bilancetti L, Becchetti E, Angeletti G, Mancuso F, Calafiore R. Encapsulation, *in vitro* characterization, and *in vivo* biocompatibility of Sertoli cells in alginate-based microcapsules. Tissue Eng 2007;13(3):641–648.
49. Elliott RB, Escobar L, Tan PLJ, Muzina M, Zwain S, Buchanan C. Live encapsulated porcine islets from a type 1 diabetic patient 9.5 yr after xenotransplantation. Xenotransplantation 2007;14(2):157–161.
50. Heo YJ, Shibata H, Okitsu T, Kawanishi T, Takeuchi S. Long-term *in vivo* glucose monitoring using fluorescent hydrogel fibers. Proc Natl Acad Sci USA 2011;108 (33):13399–13403.
51. Matsuda N, Shimizu T, Yamato M, Okano T. Tissue engineering based on cell sheet technology. Adv Mater 2007;19(20):3089–3099.
52. Yang J, Yamato M, Nishida K, Ohki T, Kanzaki M, Sekine H, Shimizu T, Okano T. Cell delivery in regenerative medicine: the cell sheet engineering approach. J Control Release 2006;116(2):193–203.
53. Langer R, Vacanti JP. Tissue engineering. Science 1993;260(5110):920–926.
54. Tsuda Y, Morimoto Y, Takeuchi S. Monodisperse cell-encapsulating peptide microgel beads for 3D cell culture. Langmuir 2010;26(4):2645–2649.
55. McGuigan AP, Sefton MV. Vascularized organoid engineered by modular assembly enables blood perfusion. Proc Natl Acad Sci USA 2006;103(31):11461–11466.
56. Du Y, Lo E, Ali S, Khademhosseini A. Directed assembly of cell-laden microgels for fabrication of 3D tissue constructs. Proc Natl Acad Sci USA 2008;105(28):9522–9527.
57. Bruzewicz DA, McGuigan AP, Whitesides GM. Fabrication of a modular tissue construct in a microfluidic chip. Lab Chip 2008;8(5):663–671.
58. Chung SE, Park W, Shin S, Lee SA, Kwon S. Guided and fluidic self-assembly of microstructures using railed microfluidic channels. Nat Mater 2008;7(7):581–587.
59. Nakamura M, Iwanaga S, Henmi C, Arai K, Nishiyama Y. Biomatrices and biomaterials for future developments of bioprinting and biofabrication. Biofabrication 2010;2 (1):014110.
60. Mironov V, Visconti RP, Kasyanov V, Forgacs G, Drake CJ, Markwald RR. Organ printing: tissue spheroids as building blocks. Biomaterials 2009;30(12):2164–2174.
61. Calvert P. Printing cells. Science 2007;318(5848):208–209.